

In End Face Milling, the Effect of Different Cooling and Lubrication Conditions on the Cutting Performance and the Surface Integrity of the Superalloy Inconel 718

Prof. Suhas Rewatkar¹, Prof. Gaurav Gohane², Prof. Dharmendra A. Agrawal³,
Prof. Hemant Baitule⁴, Yadav Jyoti Rakeshkumar⁵

^{1,2,3,4}Professor, Department Of Mechanical Engineering, J D College of Engineering & Management, Nagpur

⁵Student, Department Of Mechanical Engineering, J D College of Engineering & Management, Nagpur

ABSTRACT:

Superior thermal and mechanical qualities are shared by the nickel-based superalloy Inconel 718. However, it's a challenging material to machine since it generates a lot of heat during processing. Its cutting performance and surface integrity may be drastically improved with proper cooling and lubrication (CL) techniques. Different methods of cutting Inconel 718 are compared in this work, including dry cutting (DC), flood cutting (FC), cryogenic cutting (CC), and cryogenic minimal quantity lubrication cutting (CMQLC). Measurements include cutting forces, temperature, tool wear, chip size, roughness angle (Ra), microstructure, and residual stress (RS). The results show that processing is improved with the addition of CL. Compared to DC, CMQLC yields an average temperature that is 55.47% cooler. With CMQLC, the area of tool chipping is reduced by 25%, and the surface Ra is lowered by 32.05%, making it the lowest of the four methods. In terms of RS, while the TRS went up by 7.9%, the MCRS went up by 3.9%, and the influence depth in the subsurface went up by 10.2%. Additionally, a more desirable RS state may be attained under machining conditions with a high mechanical thermal ratio. Mild environmental contamination, favoured cutting performance, and excellent workpiece surface integrity are all shown by the CMQLC. Inconel 718, cutting performance, surface integrity, cooling and lubrication (CL), and cryogenic minimum quantity lubrication (CMQL) are some examples of relevant keywords.

1. INTRODUCTION

Inconel 718 nickel-based superalloy is widely used in aerospace engine turbine disks and blades, nuclear reactors, and other fields because of its low thermal conductivity, corrosion resistance, and anti-fatigue performance. Nevertheless, the excellent properties also make Inconel 718 one of the most difficult-to-cut materials. The cutting of Inconel 718 exhibits the characteristics of high coolant consumption, short tool life, and poor surface integrity. Although significant progress has been carried out in tools and cooling and lubrication (CL) strategies, the machining of Inconel 718 is still considered to be a huge challenge. During the cutting, about 98% of the energy is converted into heat, resulting in a significant rise in temperature at the cutting area. The addition of coolant can effectively cool the cutting zone compared to blocking heat generation¹ and reduce friction.² The machined

Table 1. Chemical composition of Inconel 718 (in % of mass).

Ni	Fe	Cr	Nb	Mo	F	Ti	Al	Ta	Co	Si	Mn
51.48	18.29	18.11	5.54	2.70	1.74	1.11	0.53	0.33	0.15	0.05	0.05

surface is usually tensile residual stress (TRS). Adding CL can reduce the TRS and produce compressive residual stress (CRS),³ increase the hardness and reduce the roughness of the surface, which can prolong the fatigue life of parts.⁴ Inconel 718 has been studied to predict the surface integrity and concluded that there is a strong correlation between roughness, fatigue life, and RS.⁵ So, it is necessary to explore the influence of the CL conditions on the cutting performance and surface integrity in Inconel 718 cutting.

CMQL is a technology that simultaneously provides cryogenic gas and lubrication oil, which reduces the cost of coolant in the cutting.⁶ Recently, the CMQL has been widely used in cutting Ti6Al4V,⁷ AISI 316L,⁸ and AISI 10459 showing the good cutting performance and surface roughness. Lubricants with low viscosity and high friction coefficient can extend tool life,¹⁰ it can even reach 200%.¹¹ Moreover, under the CMQLC, chips are easily removed with less thickness and friction.¹²

However, as much heat is generated during Inconel 718 cutting, it is uncertain whether tiny droplets can effectively enter the cutting area. Compared with traditional cutting, CMQL results in better surface integrity in grinding Inconel 718.¹³ When turning Inconel 718, the superiority of CMQL is verified by studying the tool wear, cutting forces, surface roughness,^{14,15} and microstructure.¹⁶ Although the lubricating effect is not as good as emulsion oil but can achieve more than 90% of FC, and is more environmentally friendly.¹⁷ Then, applying high-pressure coolant results in better cutting performance with less tool wear, and the adhesion wear of chips is also reduced.¹⁸ When the coolant uses a cryogenic medium, the tool life is 57% higher than that of FC and 20% of MQL at room temperature. So the CMQLC can replace the traditional method of cooling and lubrication, and realize the balance between technology and environment.^{19,20}

Most of the research on the effect of CL on Inconel 718 cutting focuses on single aspects such as tool wear or RS. And the research on the RS caused by cutting focuses on surface^{3,21} and simulation.^{22,23} There are studies on the cutting performance or surface integrity of Inconel 718,^{4,24} but the comprehensive evaluation of the two is less, especially the RS at subsurface.²⁵ Consequently, this research focuses on milling Inconel 718 under DC, FC, CC, and CMQLC, respectively. Cutting forces and temperature are measured, and the chips are analyzed.

The surface integrity is identified by measuring the surface roughness, microstructure, and RS.

Experimental setup

Workpiece properties

The experimental material is Inconel 718 after heat treatment (σ_{HV} 452). After elemental and metallographic analysis and tensile experiment of the experimental materials, the following data are obtained.²⁶ And the main chemical composition elements are shown in Table 1. The microstructure of Inconel 718 is shown in Figure 1(a), which is composed of g matrix, NbC, g#, g##, and d phases. Figure 1(b) is the stress-strain curve of Inconel 718 after heat treatment. Yield strength $\sigma_{0.2}$ is 1308.6 MPa at 20°C.

Experimental procedure

The milling experiment is carried out on the DX6080. The end surface of the workpiece with a boundary size of 18 mm \times 30 mm. And the tool is the VSM-4E(D4) of ZCC.CT (Figure 2(b)), the substrate material is cemented carbide, coated with AlTiN.

The experiment system is shown in Figure 2(a) to (c). CMQL equipment (PMPM15-S, SUNAIR, Figure 2(a)) is mainly composed of a refrigeration module and an oil mist module, with independent volume and continuous injection. High-pressure gas (4–8 bar) enters the system through the pipeline, the cryogenic air is ejected from the vortex nozzle (measurement value: 23°C). The oil mist module converts vegetable oil-based lubricant into mist (0.05–0.2 L/h) by pulse regulation and then sprayed through the nozzle. Select intermediate values according to the range of cutting parameters recommended by the tool, as shown in Table 2. Cryogenic flow with high pressure reduces cutting forces, shortens and removes chips, then reduces friction and scratch. In this system, cooling is mainly provided by compressed gas, and lubrication is provided by the oil mist.²⁷

DC does not impose any CL measures; FC is poured with cutting fluid in the cutting area. The milling model assisted by CMQL is shown in Figure 2(a) and (d). The blue area marked on the workpiece has a long and stable cutting, it is used to study the cutting performance and surface integrity.

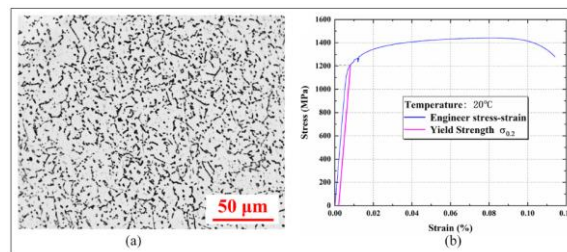


Figure 1. Microstructure and tensile properties of the Inconel 718 superalloy: (a) OM microstructure and (b) tensile stress-strain curve.

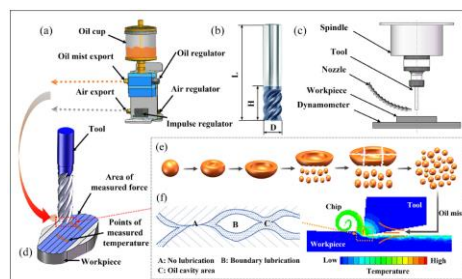


Figure 2. Experimental setup, milling, and lubrication models: (a) CMQL device (PMPM15-S), (b) tool model (VSM-4E), (c) the milling model, (d) experimental model, (e) breakage of oil droplets, and (f) lubrication model.

2. RESULTS AND DISCUSSION

Lubrication mechanism

According to the theory of liquid sprays²⁸ and fluid dynamics,²⁹ the CMQL lubrication model and the oil droplet breaking model are obtained. The breakage of oil droplets is shown in Figure 2(e). The essence of lubricant atomization is that under the external force of droplets, droplets break up and separate. In this process, external forces (such as nozzle extrusion pressure) are constantly competing with the surface tension and

Table 2. The cutting parameters.

Cutting speed (r/min)	Feed rate (mm/min)	Axial depth (mm)	Radial depth (mm)
1800	500	0.20	0.50

viscosity of droplets. Because the surface tension allows making the droplets to maintain a simple spherical, the surface energy of the whole droplets is minimized; and

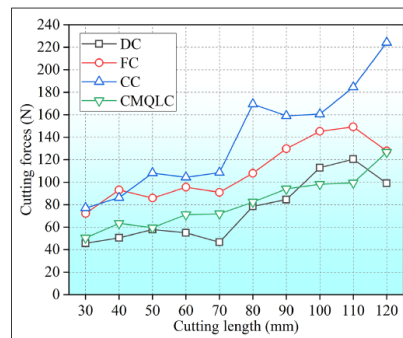


Figure 3. The variation of cutting force with the CL condition.

the viscosity of oil droplets prevents the deformation of liquid. When the external force of droplets is bigger than the surface tension and viscosity of the liquid, droplets will separate. The lubrication mechanism of CMQL is shown in Figure 2(f). It refers to that when droplets are sprayed by the nozzle, the gas vibration near the jet path will cause the vibration wave on the surface of the droplets and gradually increase. The droplets will break into flake liquid and long droplets and then into abundant smaller droplets. The size is determined by nozzle structure, jet state, and external conditions. Then, the droplets are broken and atomized, that is, under the influence of the high-speed airflow, the droplets get smaller by different crushing methods. Under external influences such as gas pressure, the droplets change into the forms of ellipsoid, cumuliform, and semi-bubble. When the velocity of the jet is higher than the threshold, the top of the semi-bubble droplets begins to break and produce annular liquid bands. The volume of the annular liquid bands is related to the size of the droplets before breaking, which enables accommodate 70% of the mass of the complete oil droplets before injection. The droplets are further crushed by the high-speed jet, and the droplets outside the jet are separated into flakes, while the droplets in the central region are cracked into plentiful microbubbles, eventually, all of the droplets are divided into microdroplets less than 2 mm.

In light of the theory of boundary lubrication film formed by coolant between two contact surfaces, the lubrication effect of oil is closely related to its volume. So the injection amount of oil mist has a great influence on the formation of the lubricating film. As shown in Figure 2(f), in the cutting area, there are no lubrication (A), boundary lubrication (B), and oil cavity area (C).

And the amount of oil mist sprayed by the CMQL is much less than that processed by the coolant. In addition, the high temperature and pressure at the tool prevent droplets from entering the contact area. So, it is hard to form complete liquid friction between the tool-chip and the tool-workpiece interface, which mostly exists in the form of boundary lubrication. Large droplets translate into the paste as they cut metal, and it tends to stick to the tool and workpiece. Smaller droplets allow penetrate the cutting zone better and cause faster

evaporation of water from the contact zone.⁹ So tiny oil droplets can reduce the friction coefficient and cutting force, providing better surface wettability.³⁰ The increase of atomized air pressure is beneficial to the increase of wetting area and leads to a significant increase in heat dissipation capacity. Therefore, the reduction of residual stress is effective.³¹ So smaller oil droplets are beneficial to cutting.

Cutting forces

Cutting forces measurement system consists of a Kistler dynamometer (9257B) and an A/D data acquisition board, a charge amplifier, a data collector, and acquisition software (DynoWare).

The change of the average cutting force with the cutting length is shown in Figure 3. Cutting forces increases sharply at 80 mm. Due to the hardness decreasing relatively at high temperatures, cutting forces of DC is relatively small, but the variation span is large. Cutting forces increase and are relatively stable in FC. Due to the big friction and severe tool wear, cutting forces are the largest and unstable under CC. The CMQLC and DC forces are smaller, but CMQLC has a more stable trend, this is because it provides excellent lubrication to reduce friction in the cutting area. Consequently, the CMQLC has relatively small and stable cutting forces.

Cutting temperature

The cutting temperature is measured using a handheld infrared thermometer testo 868. Six measure points (Figure 2) are selected with stable cutting.

The temperature variation is shown in Figure 4(a) and the average is shown in Figure 4(b). The cutting temperature is affected by tool and CL, the temperatures obtained by four CL methods all show a trend of increase. DC and CC increase greatly, while FC and CMQLC increase slightly. DC has the largest amplitude because no CL is provided. Although the CC effectively cools the cutting area, it hardly reduces the heat from friction. Larger cutting forces lead to more intense vibration and severe tool wear. The CMQLC provides oil mist, which effectively reduces friction, and further reduces tool wear. The heat is taken away by the

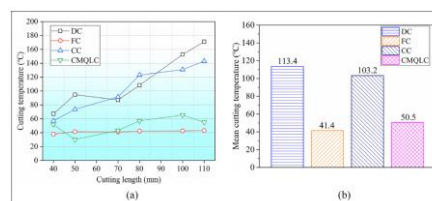


Figure 4. Cutting temperature variation with CL condition (a) and its average value (b).

coolant in a short time in FC. Whereas, due to the defects of the non-contact measurement itself, the actual cutting temperature may be higher than theirs. And the FC still has the best cooling effect and provides water lubrication; the cutting temperature under CMQLC is also acceptable, so it is necessary to add lubricating medium in the cutting of high hardness materials such as Inconel 718.

Cutting edge chipping

The wear of the tool is observed by the microscopy (EASSON-EVM2515T).

Tool wear and chipping are considered crucial parameters affecting surface integrity,⁴ which reduce the clearance angle, increase the contact area between tool and workpiece, and raise the temperature and force. The high stress caused by them is the main reason for the change in the subsurface. The high temperature will lead to the expansion and plastic deformation of work-piece materials.³²

Figure 5(a) shows the end face and flank topography of the tool. Figure 5(b) is the corresponding area of chipping. The friction between contact pairs is larger in DC, and the temperature is highest; the flank of the tool is seriously worn and the cutting edge is peeled off, the chipping area reaches 0.19 mm². The contact pairs are lubricated by the coolant in FC, which reduces friction, and takes away the cutting heat and the chips. The chipping area reduces to 0.12 mm².

The maximum of chipping is observed in CC, reaching 0.26 mm²; it contributes to the cryogenic gas providing a pre-cooling effect for contact pairs. The surface of the workpiece becomes hard, and the brittleness of the tool may increase slightly. Because no lubrication is provided, the instantaneous friction and impact force of contact pairs is large, so edge chipping occurs. In the subsequent cutting, the tool is seriously damaged and the surface quality deteriorates, which is closely related to the forces and temperature, and the rough surface. It is similar to the results obtained in Bagherzadeh et al.,⁷ so the method of only cooling without lubrication is not suitable for cutting large hardness materials such as Inconel 718.

The CMQLC availablely reduces the friction and force between the contact pairs. The chipping area is 0.09 mm². Nevertheless, the oil will adhere to some tiny chips on the surface, resulting in abrasive wear. In conclusion, CMQLC induces the slightest flank chipping, which can be considered to show the longest tool life.

Surface roughness

The 3D profile scanner InfmiteFocus G4g of ALICONA company is used to detect the surface morphologies obtained by cutting with the same parameters. The sampling length of 4 mm is selected to obtain the cloud map of the surface to calculate the Ra.

The characterization of the surface is shown in Figure 6. According to the surface topography, the surface of DC and CC has different degrees of abrasion. Severe wear and scratch determine its poor surface in CC, and the obvious groove also supports this view. And the Ra of CC is the highest, reaching 3.397, which may be because the tool is seriously broken. Although the Ra of DC is lower, its surface damage is more serious, because of big friction and high temperature. Moreover, some chips are not discharged in time. The surface topography of FC is relatively flat, without

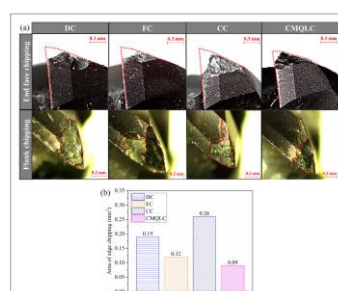


Figure 5. Tool chipping under different CL conditions: (a) topography of edge chipping and (b) areas of flank chipping.

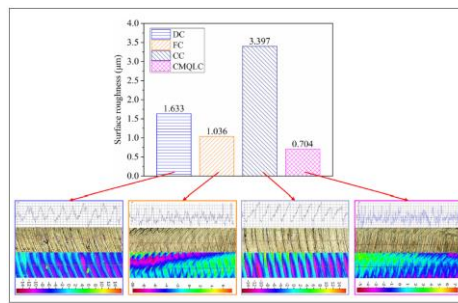


Figure 6. Surface roughness and morphology under different CL conditions.

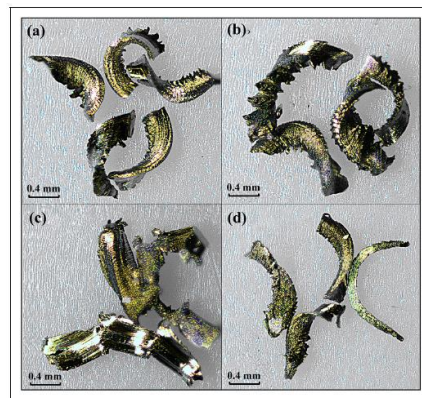


Figure 7. Chip morphology under different CL conditions:
(a) DC, (b) FC, (c) CC, and (d) CMQLC

scratches, and with less wear. Compared to DC (Ra 1.633) and FC (Ra 1.036), the CMQLC obtains relatively minimal surface roughness (Ra 0.704) due to its excellent CL effects. The surface profile generated by CMQLC may be messy because the tiny chips are adhered to the surface by oil, but CMQLC is still considered to be the best way.

Chip morphology

The chip morphology is also observed by microscopy. The temperature of the cutting area depends on heat production and dissipation. The dominant position of mechanical load and thermal effect for machining deformation depends on the heat dissipation capacity of the chip, and the improvement of material removal rate is beneficial. As a result, chip morphology has a paramount influence on surface integrity.³³

Figure 7 shows the chip morphologies. When using DC, chips are more uniform with serrated edges. The formation mechanism of a serrated edge is that the increasing pressure in the shear zone leads to the decrease of shear angle and the shear plane transforms into a shear body. When the material reaches the strain limit, cracks appear on the free surface and adiabatic shear occurs along the crack direction. Under the combined action of cracks and adiabatic shear, serrated chips are generated. When pouring coolant, the chip has a spiral trend, the curling degree is reduced, the length is slightly increased, and the serrated edge of the chip is increased. This may be because the lower temperature is not enough to make the chip produce large bending, so the chip length is longer when the chip

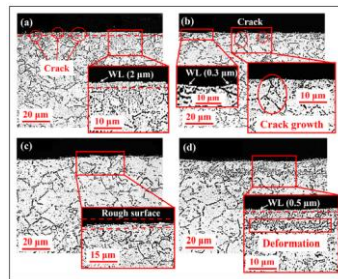


Figure 8. The metallographic structure under different CL conditions: (a) DC, (b) FC, (c) CC, and (d) CMQLC.

breaks. When using the cryogenic method, the chip no longer presents regular morphology but appears extrusion chip with fewer or no serrated edges. The chip brittleness increases at low temperatures, and it is easier to break. Nevertheless, the cutting edge of the tool with large wear is blunt, and the chips are mainly caused by extrusion and cracking. When the CMQL method is adopted, the chip is narrow, the curling degree is small, and the edge sawtooth is not obvious. The chip-breaking performance is good at low temperatures, the friction force under oil mist lubrication is small, and the squeezing effect is weakened. This type of chip facilitates material removal and reduces surface damage.

Microstructure

The microstructure is observed under a metallographic microscope (Leica DM2700 M) and SEM (ZEISS EVO 18), and the sample surface is mechanically ground and polished to study the metallographic structure in the subsurface.

It is found from Pusavec et al.⁴ that there is no significant change in the fiber structure with small cutting strength. However, the mechanical effect plays a dominant role in cryogenic cutting, and grain plastic deformation is mainly related to tool wear and cutting force.³⁴ The more serious the tool wear, the greater cutting forces, and the more obvious the grained plastic deformation. The processing-induced white layer (WL) is the possible adverse surface integrity characteristic.³⁵ The metallographic microstructure is shown in Figure 8. The WL (2 mm) appears under the DC, which means that WL is more likely to form at higher temperatures and worn tools; small cracks appeared on the surface, some grain crushing appeared on the subsurface, and

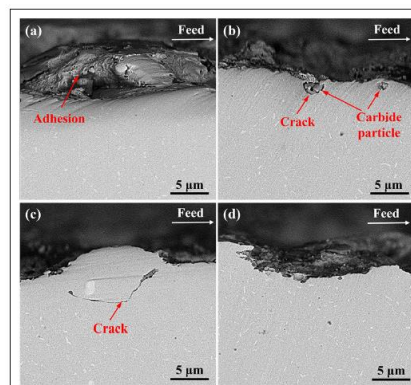


Figure 9. The metallographic structure under different CL conditions: (a) DC, (b) FC, (c) CC, and (d) CMQLC.

the plastic deformation layer (PDL) is not apparent, it is more like a layer of dynamically recovery microstructure. WL decreased to about 0.3 mm in FC, but cracks appeared on the surface and extended deeper into the interior. Under CC, because the tool is seriously damaged, the cutting process is irregular, the damaged surface is rough and the surface integrity is worse, and the microstructure shows no obvious cutting characteristics. There are few surface cracks under CMQLC, and the WL is about 0.5 mm deep; obvious plastic deformation occurs in the subsurface grains, and the depth of the PDL is about 13 mm, it is more like dynamically recrystallized microstructure. This is because the mechanical effect is more dominant, and grain plastic deformation is mainly related to tool wear and cutting force.³⁴ The depth of the WL can be significantly reduced by using coolant, and the PDL can be obtained by using CMQL, which helps to improve fatigue life.

The SEM images of the cross-section of the workpiece after processing are shown in Figure 9. In DC, the adhesion phenomenon occurs. This is due to the material affinity becoming larger under high temperatures, and cold welding occurs, so the material adheres to the surface of the workpiece. The use of FC reduces the phenomenon of adhesion, but cracks appear at hard particles. Under CC, due to the chipping of the tool and the absence of a lubricating medium, a large mechanical load is generated, so cracks appear on the subsurface and have a tendency to expand. With CMQL, both chipping and crack are decreased, providing advantages for reducing surface cracking and increasing fatigue life.

Residual stress

The RS is measured by X-Ray Diffraction (Bruker, D8), using the $\sin^2\psi$ method and the Mn target. Five measuring points are taken on each plan and then take the average. The electrolyte is mixed with CH₃OH (90%) and HClO₄ (10%), and the depth of each electrolysis is 5 mm.

The RS is mainly caused by uneven plastic deformation in cutting. The CRS is usually beneficial, and the TRS is usually harmful, which will reduce structure yield strength. The RS also plays an important role in the working properties of materials, especially fatigue life, crack corrosion, fracture, and wear resistance properties.³⁶

The thermal effect leads to TRS on the surface, while the mechanical effect leads to CRS.³⁷ The variation of the RS with depth is shown in Figure 10(a). It is

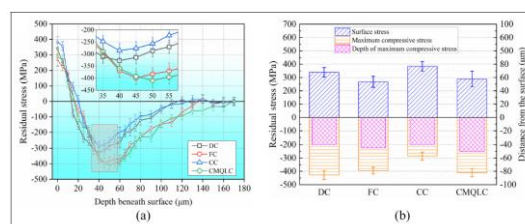


Figure 10. Residual stress under different CL conditions: (a) variation trend and (b) stress characterization.

observed that the surface stress is always TRS, and it of FC and CMQLC is lower; the RS in the subsurface is mainly CRS, which is the result of the increase of mechanical load and plastic deformation flow. The TRS decreases rapidly and transforms into CRS at about 20 mm depth, and CRS increases rapidly with the increase of depth. DC, FC, CC, and CMQLC reach the maximum compressive residual stress (MCRS) at 40, 45, 40, and 50 mm below the

surface, respectively. Among them, the CRS reached by DC is the largest, followed by CMQLC, FC, and CC.

When the Ra is relatively small and the CRS amplitude value is bigger, it possesses preferable anti-fatigue capability. CMQL has the smallest Ra (0.704) and a relatively large CRS amplitude value (2409.43 MPa). So, this is a way to provide excellent fatigue resistance. In addition, the larger the MCRS and the deeper the position, and the smaller the TRS on the surface, as a characterization reference with good TRS (Figure 10(b)). A weight parameter l is proposed to represent the above characterization reference, it is calculated by formula (1). The four CL methods are 1.68, 1.75, 1.10, and 2.02, respectively. The larger l is, the more effective the RS increases the life of components.

$$\lambda = (R_{s_{\max_compressive}} \cdot Depth - R_{s_{surface}}) \cdot 10^{-4} \quad (1)$$

where $R_{s_{\max_compressive}}$ is the MCRS, MPa; Depth is the depth of MCRS, mm; $R_{s_{surface}}$ is the RS on the surface, MPa.

On the other hand, cutting force and temperature influence surface RS. The force-heat ratio e is calculated by Formula (2), and the e is respectively to DC (0.662), FC (2.650), CC (1.339), and CMQLC (1.617).

It is observed that a high e is beneficial to reducing TRS, and has a bigger CRS and depth. It should be noted that although FC has the highest e , it is associated with increased coolant costs and environmental problems. Whereas, for the case of high temperature caused by severe tool wear under cryogenic conditions, TRS may increase accordingly, and the increasing rate of CRS is high with depth increasing, which is the same as the results obtained in Bagherzadeh et al.⁷ It can be assumed that the cutting conditions with a higher e are effective in extending the fatigue life of the workpiece.²²

$$e = \frac{\sum F_1 + F_2 + \dots + F_n}{nT} \quad (2)$$

Where F_1 – F_n is the average cutting force of n measuring areas, N; t is the average cutting temperature, °C. By considering the effect of residual stress on fatigue life, the cost of coolant, and environmental protection, CMQL is the optimized CL condition for cutting Inconel 718 superalloy.

3. CONCLUSION

To improve the machining efficiency and service life of Inconel 718 parts, the cutting performance and surface integrity of Inconel 718 in four CL modes of DC, FC, CC, and CMQLC are compared and analyzed. The main conclusions are as follows:

(1) The CMQLC offers the best overall cutting performance compared to the other three methods. Cutting forces obtained under CMQLC are smaller and more stable. The average cutting temperature is 55.47% lower than that of DC. The chips are short and non-serrated, which are effectively discharged with little scratch to the surface. And the tool chipping area is the smallest, which is further reduced by 25% compared with FC.

(2) The CMQL has a distinct advantage in the surface integrity achieved by cutting Inconel 718. The Ra obtained under the CMQL condition is the lowest, which is 32.05% lower than that of FC. The thickness of the white layer is 0.5 mm, and the PDL is about 13

mm deep. Although the TRS obtained by CMQLC is 7.9% larger than that of FC, the subsurface MCRS and influence depth obtained by CMQLC are larger, increasing by 3.9% and 10.2% respectively. And the cutting conditions with a larger force-heat ratio enable obtaining better RS on the surface and below, to obtain better fatigue life.

(3) The FC provides a better cooling effect and a lot of heat is taken away by the flowing coolant. The lubrication of oil mist provided by CMQL allows making the surface adhere to tiny chips, resulting in small scratches. However, it has little effect on the overall surface roughness and still has the best surface finish. Another concern is that cryogenic gas pre-cools the cutting area and no lubrication is provided, the tool suffered severe wear and chipping. As a result, the processing of high-hardness materials is not suitable for the condition of only cooling without lubrication.

(4) With the cutting performance and surface integrity analyzed, CMQL has the best comprehensive performance in cutting Inconel 718, examples include reduced coolant cost, prolonged tool life, reduced surface roughness, and preferred CRS distribution.

Declaration of conflicting interests

The author(s) declared no potential conflicts of interest with respect to the research, authorship, and/or publication of this article.

Funding

The author(s) disclosed receipt of the following financial support for the research, authorship, and/or publication of this article: This work was supported financially by the Important National Science and Technology Specific Projects (No.2018ZX04040001) and the Shanghai Sailing Program (No.17YF1403100).

4. REFERENCES

1. Mia M, Rahman MA, Gupta MK, et al. Advanced cooling-lubrication technologies in metal machining. In: Pramanik A (ed.) *Machining and tribology*. Amsterdam: Elsevier, 2022, pp.67–92.
2. Anand N, Kumar AS and Paul S. Effect of cutting fluids applied in MQCL mode on machinability of Ti-6Al-4V. *J Manuf Process* 2019; 43: 154–163.
3. Arunachalam RM, Mannan MA and Spowage AC. Residual stress and surface roughness when facing age hardened Inconel 718 with CBN and ceramic cutting tools. *Int J Mach Tools Manuf* 2004; 44: 879–887.
4. Pusavec F, Hamdi H, Kopac J, et al. Surface integrity in cryogenic machining of nickel based alloy—Inconel 718. *J Mater Process Technol* 2011; 211: 773–783.
5. Holmberg J, Wretland A, Hammersberg P, et al. Surface integrity investigations for prediction of fatigue properties after machining of alloy 718. *Int J Fatigue* 2021; 144: 106059.
6. Sharma VS, Dogra M and Suri NM. Cooling techniques for improved productivity in turning. *Int J Mach Tools Manuf* 2009; 49: 435–453.
7. Bagherzadeh A, Kuram E and Budak E. Experimental evaluation of eco-friendly hybrid cooling methods in slot milling of titanium alloy. *J Clean Prod* 2021; 289: 125817.
8. Szczotkarz N, Mrugalski R, Maruda RW, et al. Cutting tool wear in turning 316L stainless steel in the conditions of minimized lubrication. *Tribol Int* 2021; 156: 106813.

9. Maruda RW, Krolczyk GM, Feldshtein E, et al. Tool wear characterizations in finish turning of AISI 1045 carbon steel for MQCL conditions. *Wear* 2017; 372–373: 54–67.
10. Pereira O, Martín-Alfonso JE, Rodríguez A, et al. Sustainability analysis of lubricant oils for minimum quantity lubrication based on their tribo-rheological performance. *J Clean Prod* 2017; 164: 1419–1429.
11. Chen J, Yu W, Zuo Z, et al. Tribological properties and tool wear in milling of in-situ TiB₂/7075 Al composite under various cryogenic MQL conditions. *Tribol Int* 2021; 160: 107021.
12. Maruda RW, Krolczyk GM, Nieslony P, et al. Chip formation zone analysis during the turning of austenitic stainless steel 316L under MQCL cooling condition. *Procedia Eng* 2016; 149: 297–304.
13. Naskar A, Singh BB, Choudhary A, et al. Effect of different grinding fluids applied in minimum quantity cooling-lubrication mode on surface integrity in cBN grinding of Inconel 718. *J Manuf Process* 2018; 36: 44–50.
14. Ostrowicki N, Kaim A, Gross D, et al. Effect of various cooling lubricant strategies on turning Inconel 718 with different cutting materials. *Procedia CIRP* 2021; 101: 350–353.
15. Gupta MK, Mia M, Pruncu CI, et al. Parametric optimization and process capability analysis for machining of nickel-based superalloy. *Int J Adv Manuf Technol* 2019; 102: 3995–4009.
16. Marques A, Paipa Suarez M, Falco Sales W, et al. Turning of Inconel 718 with whisker-reinforced ceramic tools applying vegetable-based cutting fluid mixed with solid lubricants by MQL. *J Mater Process Technol* 2019; 266: 530–543.
17. Pereira O, Catala P, Rodríguez A, et al. The use of hybrid CO₂ + MQL in machining operations. *Procedia Eng* 2015; 132: 492–499.
18. Polvorosa R, Suárez A, de Lacalle LNL, et al. Tool wear on nickel alloys with different coolant pressures: comparison of Alloy 718 and Waspaloy. *J Manuf Process* 2017; 26: 44–56.
19. Pereira O, Celaya A, Urbikain G, et al. CO₂ cryogenic milling of Inconel 718: cutting forces and tool wear. *J Mater Res Technol* 2020; 9: 8459–8468.
20. Pereira O, Urbikain G, Rodríguez A, et al. Internal cryo-lubrication approach for Inconel 718 milling. *Procedia Manuf* 2017; 13: 89–93.
21. Boozarpoor M, Teimouri R and Yazdani K. Comprehensive study on effect of orthogonal turn-milling parameters on surface integrity of Inconel 718 considering production rate as constrain. *Int J Lightweight Mater Manuf* 2021; 4: 145–155.
22. Jiang X, Kong X, He S, et al. Modeling the superposition of residual stresses induced by cutting force and heat during the milling of thin-walled parts. *J Manuf Process* 2021; 68: 356–370.
23. Vovk A, Söller J and Karpuschewski B. Finite element simulations of the material loads and residual stresses in milling utilizing the CEL method. *Procedia CIRP* 2020; 87: 539–544.
24. Jeyapandiarajan P and Anthony XM. Evaluating the machinability of Inconel 718 under different machining conditions. *Procedia Manuf* 2019; 30: 253–260.
25. De Bartolomeis A, Newman ST, Jawahir IS, et al. Future research directions in the machining of Inconel 718. *J Mater Process Technol* 2021; 297: 117260.

26. Yao SL, Lei XL, Wang RZ, et al. A novel cold expansion process for improving the surface integrity and fatigue life of small-deep holes in Inconel 718 superalloys. *Int J Fatigue* 2022; 154: 106544.
27. da Silva LR, Bianchi EC, Fuisse RY, et al. Analysis of surface integrity for minimum quantity lubricant—MQL in grinding. *Int J Mach Tools Manuf* 2007; 47: 412–418.
28. Cao J. *Liquid sprays*. Beijing: Peking University Press, 2013, pp.233–321.
29. Yaxiong Y. *Theories and applications of multiphase flow dynamics in high temperature and high pressure*. Beijing: Beijing Institute of Technology Press, 2016, pp.160–192.
30. Maruda RW, Krolczyk GM, Feldshtein E, et al. A study on droplets sizes, their distribution and heat exchange for minimum quantity cooling lubrication (MQCL). *Int J Mach Tools Manuf* 2016; 100: 81–92.
31. Shiva Sai S, ManojKumar K and Ghosh A. Assessment of spray quality from an external mix nozzle and its impact on SQL grinding performance. *Int J Mach Tools Manuf* 2015; 89: 132–141.
32. Zhou JM, Bushlya V, Peng RL, et al. Effects of tool wear on subsurface deformation of nickel-based superalloy. *Procedia Eng* 2011; 19: 407–413.
33. Dong G, Zhaopeng H, Rongdi H, et al. Study of cutting deformation in machining nickel-based alloy Inconel 718. *Int J Mach Tools Manuf* 2011; 51: 520–527.
34. Chaabani S, Arrazola PJ, Ayed Y, et al. Comparison between cryogenic coolants effect on tool wear and surface integrity in finishing turning of Inconel 718. *J Mater Process Technol* 2020; 285: 116780.
35. Brown M, M'Saoubi R, Crawforth P, et al. On deformation characterisation of machined surfaces and machining-induced white layers in a milled titanium alloy. *J Mater Process Technol* 2022; 299: 117378.
36. James MN. Residual stress influences on structural reliability. *Eng Fail Anal* 2011; 18: 1909–1920.
37. Pawade RS, Joshi SS and Brahmanekar PK. Effect of machining parameters and cutting edge geometry on surface integrity of high-speed turned Inconel 718. *Int J Mach Tools Manuf* 2008; 48: 15–28.
38. Cheng M, Jiao L, Yan P, et al. Prediction of surface residual stress in end milling with Gaussian process regression. *Measurement* 2021; 178: 109333